Correlation of Miscibility and Mechanical Properties of Polypropylene/Olefin Block Copolymers: Effect of Chain Composition

Guoming Liu,[1] Xiuqin Zhang,[1] Xiuhong Li,[2] Hongyu Chen,[3] Kim Walton,[4] Dujin Wang[1]

[1]*Beijing National Laboratory for Molecular Sciences, CAS Key Laboratory of Engineering Plastics, Institute of Chemistry, Chinese Academy of Sciences, Beijing 100190, China*
[2]*Shanghai Synchrotron Radiation Facility, Shanghai Institute of Applied Physics, Chinese Academy of Sciences, Shanghai 201204, China*
[3]*The Dow Chemical (China) Company Limited, Shanghai 201203, China*
[4]*The Dow Chemical Company, Freeport, Texas 77541, USA*

Received 22 February 2011; accepted 29 September 2011
DOI 10.1002/app.36244
Published online 26 December 2011 in Wiley Online Library (wileyonlinelibrary.com).

ABSTRACT: This study examines the miscibility and mechanical properties of isotactic polypropylene (iPP) and olefin block copolymer (OBC) blends (70/30 wt %). The blends exhibit phase-separated morphology. The OBC domain size decreases with increasing the 1-octene content in the soft segment. The crystallization, melting behavior, and the long spacing of the iPP component in the blends are nearly the same as those of neat iPP, while the T_g of the iPP component shifts slightly to lower temperature. "Blocky" OBC is immiscible with iPP, while the soft segment rich polymers in OBC could be partially miscible with iPP. The impact strength of the blends is greatly increased with increasing the 1-octene content in the OBC soft segment. © 2011 Wiley Periodicals, Inc. J Appl Polym Sci 125: 666–675, 2012

Key words: olefin block copolymer; isotactic polypropylene; blends; toughening; miscibility

INTRODUCTION

Rubber or elastomer toughening of semicrystalline polymers has been a traditional, but lively topic for modifying semicrystalline polymers having scientific interest and practical applications. Because of the relatively poor impact strength of isotactic polypropylene (iPP), the toughening by elastomers, such as natural rubber, ethylene-propylene rubber (EP), and EP-diene terpolymer (EPDM), has been studied extensively.[1–4] Using "single-site" metallocene catalysts, pelletized ethylene-α-olefin random copolymers, with narrow branching distribution and molecular weight distribution can impart toughening of iPP with processing ease.[5,6] The miscibility/compatibility between iPP and elastomer is one of the key concerns, which govern the ultimate mechanical properties. Yamaguchi et al. studied the compatibility of binary blends of iPP with metallocene-based random EP, ethylene-1-butene (EB), and ethylene-1-hexene (EH) copolymers[7] and found that the EPs with a propylene content of lower than 67 mol % were immiscible with iPP, while EB and EH could achieve miscibility with iPP by dissolving in the amorphous phase of iPP as the α-olefin comonomer content increased above 50 mol %. Nitta et al. further studied iPP/EP blends[8] and found that EP copolymers with a propylene content above 84 mol % were miscible with iPP, and the crystallizable PP sequences in these EP copolymers were incorporated in crystal lattice of iPP and the other portions in the EP chains were excluded to the amorphous phases, while the EP copolymers with a propylene-unit content of less than 77 mol % were incompatible with iPP. Maeder et al. studied the influence of comonomer content on the morphology and mechanical properties of iPP/metallocene-EB blends[9] and found that with increasing the 1-butene content in EB, the compatibility of iPP/EB blends was improved, resulting in better dispersion of EB and stronger interfacial adhesion; more specifically, a single phase was observed at a 1-butene content exceeding 69.9 mol %. Maeder further noted that the iPP/EB blends exhibited optimum impact toughness when an EB with a 1-butene content of 31.6 mol % was used. This suggests that there is an optimum α-olefin

Correspondence to: D. Wang (djwang@iccas.ac.cn).
Contract grant sponsors: Dow Chemical Company, National Natural Science Foundation of China; contract grant numbers: 50903089, 21074141.
Contract grant sponsor: China National Funds for Distinguished Young Scientists; contract grant number: 50925313.

TABLE I
Characteristics of OBC Samples

Sample code	Density (g/cm^3)	MFI[a] (g/10 min)	M_n (kg/mol)	Octene content in soft segment[b] (mol %)	Octene content in hard segment[b] (mol %)	Hard segment (wt %)	$X_{c,\ \Delta H}$[c] (wt %)
OBC-1	0.867	0.32	76	22.6	1.13	16	10
OBC-2	0.863	0.32	78	29.7	1.60	15	7.8
OBC-3	0.863	0.34	74	35.7	2.06	18	7.8

[a] Melt flow index, 190°C/2.16 kg.
[b] Determined from ^{13}C-NMR.
[c] Determined by enthalpy of fusion.

content in random ethylene/α-olefins copolymers for maximum iPP impact toughness. It should be noted that at the optimum α-olefin level for the study in reference,[9] the random copolymer was amorphous. Using the PRISM theory proposed by Schwiezer and Singh,[10] Lohse predicted the miscibility of polypropylene and ethylene-α-olefin copolymer blends.[11] The results showed that a "miscibility gap" exists, and ethylene-1-octene copolymer (EO) would be miscible with polypropylene at a lower weight fraction comonomer than EP. To summarize, the comonomer type and content in ethylene-based elastomer influences the miscibility and mechanical properties of iPP/elastomer blends.

Recently, the Dow Chemical Company developed the chain shuttling catalyst technology which can be used to produce olefin block copolymers (OBCs) in a continuous process.[12] The block copolymers synthesized by chain shuttling technology consist of highly crystalline ethylene-octene blocks and low crystallinity or amorphous ethylene-octene blocks. The highly crystalline blocks have very low comonomer content and high melting temperature, while the low crystallinity or amorphous blocks have high comonomer content and low glass transition temperature. This new kind of OBC has a statistical multiblock architecture with a most probable distribution in block lengths and the number of blocks per chain. When compared with random ethylene-octene copolymers, the block architecture imparts a substantially higher melting temperature and a higher crystallization temperature, while maintaining a lower glass transition temperature and a more highly organized crystalline morphology.

In the present research, it is hypothesized that the soft segment composition of OBC can be tuned to control compatibility with iPP, while the hard segments, having similar chain architecture to linear low density polyethylene (LLDPE), are expected to be incompatible with iPP.[13–16] A recent study showed that chain blockiness had an influence on the phase behavior of EO copolymer blends.[17] In a previous study,[18] we reported that OBC had better compatibility with iPP than random EO with similar density and crystallinity. However, the effect of comonomer content in soft segments on the miscibility and mechanical properties of iPP/OBC blends had not been studied. It is expected that studying the effect of the soft segment composition in OBC will lead to a better understanding of the toughening mechanism of this class of polyolefin elastomers in iPP.

EXPERIMENTAL

iPP with a melt flow rate of 35 g/10 min at 230°C/2.16 kg and three ethylene-octene block copolymers were supplied by the Dow Chemical Company. All of the OBCs have similar molecular weight and molecular weight distribution. Similar amounts of chain shuttling agent were used during production; therefore, the speculated block length and distribution of the OBCs were expected to be similar. The most distinct difference among these OBCs was the 1-octene content in the soft segment. The molecular information of OBCs is shown in Table I.

The iPP/elastomer blends (70/30 w/w) were prepared using a corotating twin screw extruder (ZSK-25, D = 25 mm and L/D = 48) operated at 200°C and a screw rotation speed of 500 rpm. Separate computer-controlled, loss-in-weight feeders were used to feed the two pelletized ingredients. An antioxidant (Irganox^{TM} B225) was added to the blends with a weight fraction of 0.2% to avoid degradation during processing. The resulting pellets were injection molded in a Yizhimi UN120A injection molding machine. A general purpose screw was used in the barrel, with barrel temperatures set at 180, 200, 200, and 210°C from the hopper to the nozzle, respectively. Three types of specimens were made: dog-bone tensile bars with width of 3.2 mm and thickness of 3.2 mm (ASTM D638 Type V); flexural test bars with dimensions of 54.5 × 6 × 4 mm^3; Izod impact test bars with length of 63.5 mm, width of 12.7 mm (10.16 mm under the notch), and thickness of 4 mm.

A JSM-6700F JEOL scanning electron microscope (SEM), operated at 5 kV, was utilized to examine the phase morphology of iPP/OBC blends. All SEM

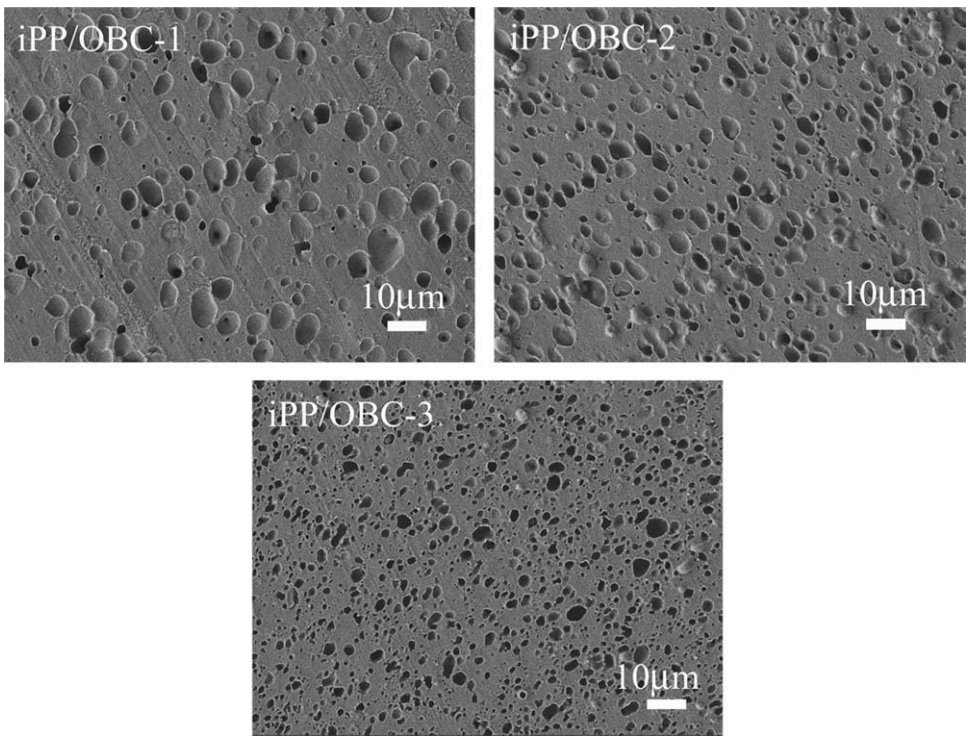

Figure 1 SEM images of iPP/OBC blends.

specimens were coated with gold of ~ 5-nm-thick to avoid charging; thereby, improving image quality. Undeformed molded specimens were examined to obtain a survey of elastomer domain size and dispersion. For this purpose, the samples were microtomed at −100°C to obtain a flat surface. The resulting surface was etched with xylene at 60°C to remove the elastomer phase from the iPP matrix. Additionally, SEM was also used to study the morphology of fracture surface of the Izod impact specimens.

The melting and crystallization behaviors of iPP/OBC blends were examined with a Perkin-Elmer differential scanning calorimeter (DSC7). The instrument was calibrated by indium before measurement. The heating and cooling scans were performed in the temperature range from 40 to 200°C at a heating or cooling rate of 10°C/min under nitrogen atmosphere with the sample weight of about 2 ~ 4 mg.

Small angle X-ray scattering (SAXS) measurements were carried out at the beamline BL16B1 in the Shanghai Synchrotron Radiation Facility (SSRF). The wavelength of the radiation source is 1.24 Å. The SAXS pattern was collected by a MAR CCD (MAR-USA) detector, which had a resolution of 2048 × 2048 pixels (pixel size = 79 × 79 μm^2). The image acquisition time was 300 s for each sample. The sample-to-detector distance was 3117.4 mm (calibrated by a biophysical standard, bull collagen). After background scattering subtraction, and correction for X-ray absorption and sample thickness, the 2D SAXS patterns were converted to one-dimensional data. The superposed scattering curves of iPP and OBC (considering the volume fraction of each component) were compared with the scattering curves of iPP/OBC blends.

The relaxation of iPP/OBC blends and pure components were examined in tensile mode in a TA DMA Q800 instrument. Films with a thickness of about 0.5 mm and width of 5 mm were prepared by compression. Temperature scans were collected in the range of −120 to 150°C, with a frequency of 1 Hz and strain of 0.05%.

The tensile experiments were performed on an Instron 3365 universal mechanical testing machine at room temperature (26°C, 55% relative humidity) with a crosshead speed of 50 mm/min. Flexural measurements were performed on an Instron 3365 universal mechanical testing machine at room temperature with a crosshead speed of 2 mm/min. The notched specimens were tested on an Izod impact machine CSI-137C at ambient temperature. The reported values of all the mechanical properties have been averaged over at least five independent measurements. For impact tests, at least 10 independent measurements were averaged.

RESULTS AND DISCUSSION

Morphologies

The solid morphologies of iPP/OBC blends were observed by SEM (Fig. 1). The blends showed a

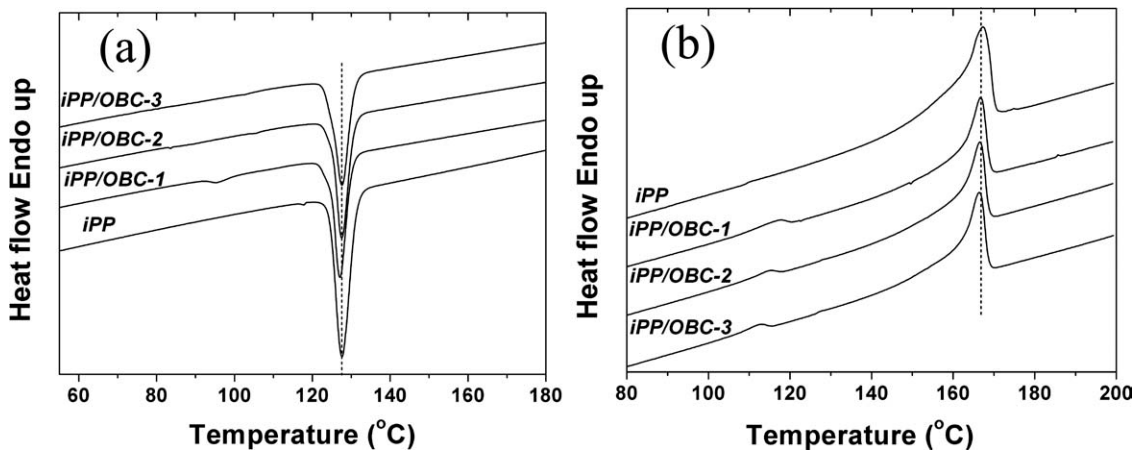

Figure 2 DSC cooling (a) and heating (b) curves of iPP and iPP/OBC blends.

phase-separated morphology with OBCs as the dispersed phase and iPP as the continuous phase. With increasing the 1-octene content in the soft segment of OBC from iPP/OBC-1 to iPP/OBC-3, the size of elastomer phase decreased remarkably. The elastomer phase size is 5.8 ± 1.5 μm, 4.7 ± 1.2 μm, and 2.6 ± 0.7 μm for iPP/OBC-1, iPP/OBC-2, and iPP/OBC-3, respectively.

The formation of dispersed phase during melt blending of polymer blends has been studied extensively.[19–21] There are two factors determining the morphology of immiscible polymer blends: the viscosity ratio $p = \eta_d/\eta_m$ (η_d: viscosity of the dispersed phase, η_m: viscosity of the matrix phase) and interfacial tension. The dispersed particle size is proportional to interfacial tension and $P^{0.84}$ when $P > 1$ or $P^{-0.84}$ when $P < 1$.[19] Therefore, binary blends with the lowest interfacial tension and a viscosity ratio close to unity would form the smallest dispersed phase particles. The three OBCs have similar MFI, thus the viscosity for the three blends is expected to be similar. Therefore, it is likely that the dominant controlling factor for dispersed phase size in the blends is the iPP/OBC interfacial tension. SEM observations of decreasing OBC average particle size with increasing soft segment 1-octene content implied that the compatibility between iPP and OBC increased with increasing soft segment 1-octent content, by reducing the interfacial tension between the two components.

Crystallization and melting behaviors

The crystallization and melting behaviors of the blends were investigated by DSC. As shown in the cooling curves [Fig. 2(a)], exothermic peaks at around 127°C correspond to the crystallization of iPP component. For iPP/OBC-1, a small exothermic peak can be found at about 95°C, which can be identified as the crystallization of OBC. No crystallization peak of OBC in iPP/OBC-2 or iPP/OBC-3 was observed. A major endothermic peak located at about 165°C corresponding to the melting of iPP component was observed in the second heating curves of neat iPP and iPP/OBC blends [Fig. 2(b)]. Additionally, a small peak at about 117°C can be seen in all the three blends, corresponding to the melting of the OBCs. The crystallization peaks of OBC in iPP/OBC-2 and 3 were not detected, possibly because the net crystallinities of OBC-2 and 3 were lower than that of OBC-1 (Table I). Therefore, the heat flow of the primary crystallization process of OBC-2 and 3 in the blends is too small to be detected by the instrument.

The crystallinity of the iPP component was calculated from the ratio of the fusion enthalpy per normalized gram of iPP in the blend to that of a theoretically 100% crystalline iPP (taken as 209 J/g).[22] The crystallization temperatures, melting temperatures, and crystallinities of iPP component in the blends are similar (Table II). Some literatures indicated that the elastomer phase could act as a nucleating agent for iPP crystallization, resulting in a

TABLE II
Crystallization/Melting Temperatures and Crystallinity of iPP Component in Neat iPP and iPP/OBC Blends

Sample	iPP	iPP/OBC-1	iPP/OBC-2	iPP/OBC-3
T_c (°C)	127.6 ± 0.1	127.1 ± 0.1	127.5 ± 0.1	127.5 ± 0.1
T_m (°C)	167.2 ± 0.1	166.7 ± 0.1	166.5 ± 0.1	166.4 ± 0.1
Crystallinity (%)	52 ± 1	50 ± 1	51 ± 1	52 ± 1

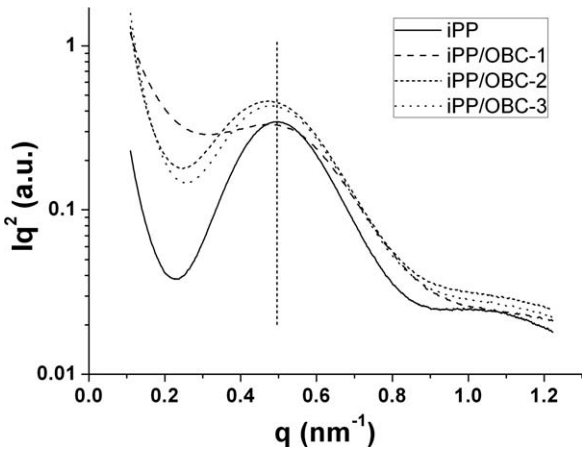

Figure 3 Small angle X-ray scattering curves of neat iPP and iPP/OBC blends.

decrease of melting temperature and an increase of crystallization temperature.[3] Some other reports showed that the random EO phase had almost no influence on the crystallization[23] or melting[24] behaviors of iPP. Whether the crystallization of iPP was influenced depends on the miscibility and the composition of the blends. The spherulite growth rate decreases in miscible blends compared with pure iPP due to a dilution effect, but it is almost unchanged in immiscible blends.[8] Composition is another important factor. When the iPP phase is the dispersed phase, the crystallization in isolated regions will occur at a lower temperature due to the reduction of the average heterogeneous nuclei.[25–27] These results suggested that these iPP/OBC blends were immiscible.

Small angle X-ray scattering

SAXS usually was applied to characterize the long spacing (L), crystalline layer thickness (l_c), and amorphous layer thickness (l_a) of semicrystalline polymers. For two crystalline polymer blends, a single long spacing peak in the blends was ascribed to be miscible while two separate peaks were an indication of segregation.[28,29] For iPP blends with amorphous elastomers, an increase of L or l_a was usually thought to be the result that the elastomer was incorporated in the amorphous layer of iPP.[7,8,30] The Lorentz-corrected SAXS curves of neat iPP and iPP/OBC blends are plotted in Figure 3. Neat iPP and iPP/OBC-2 and -3 show distinct long spacing peaks. The maxima of the peaks located at lower q than that of iPP, indicating that the blends had larger long spacings than iPP. The long spacing peak of iPP/OBC-1 was a shoulder peak with the maximum location near the same q as that of iPP. It seems that the results are similar with the previous reports on

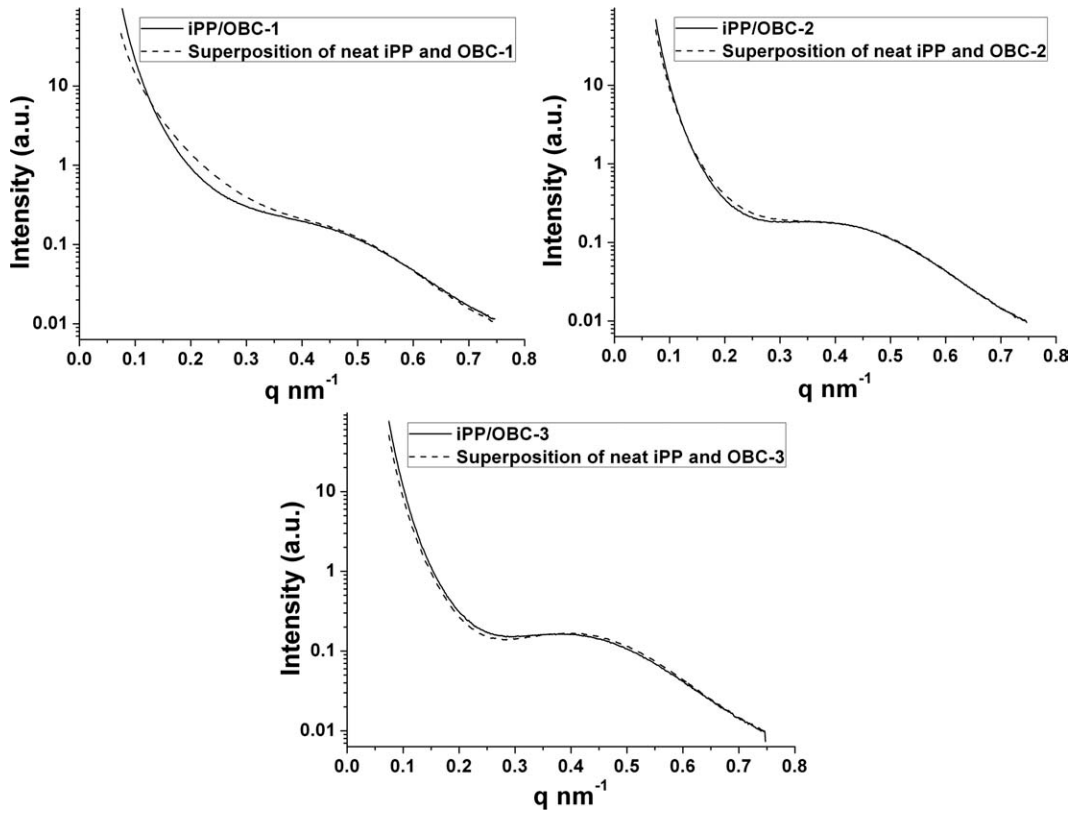

Figure 4 Comparison of experimental SAXS curves of iPP/OBC blends and the superposition results of the two components.

TABLE III
The Apparent Long Spacings of iPP/OBC Blends and Superposed iPP and OBC Curves

	iPP	iPP/OBC-1	iPP/OBC-2	iPP/OBC-3
Experimental L (nm)	13.2	13.8	13.8	13.6
Superposed L (nm)	–	13.7	13.8	13.6

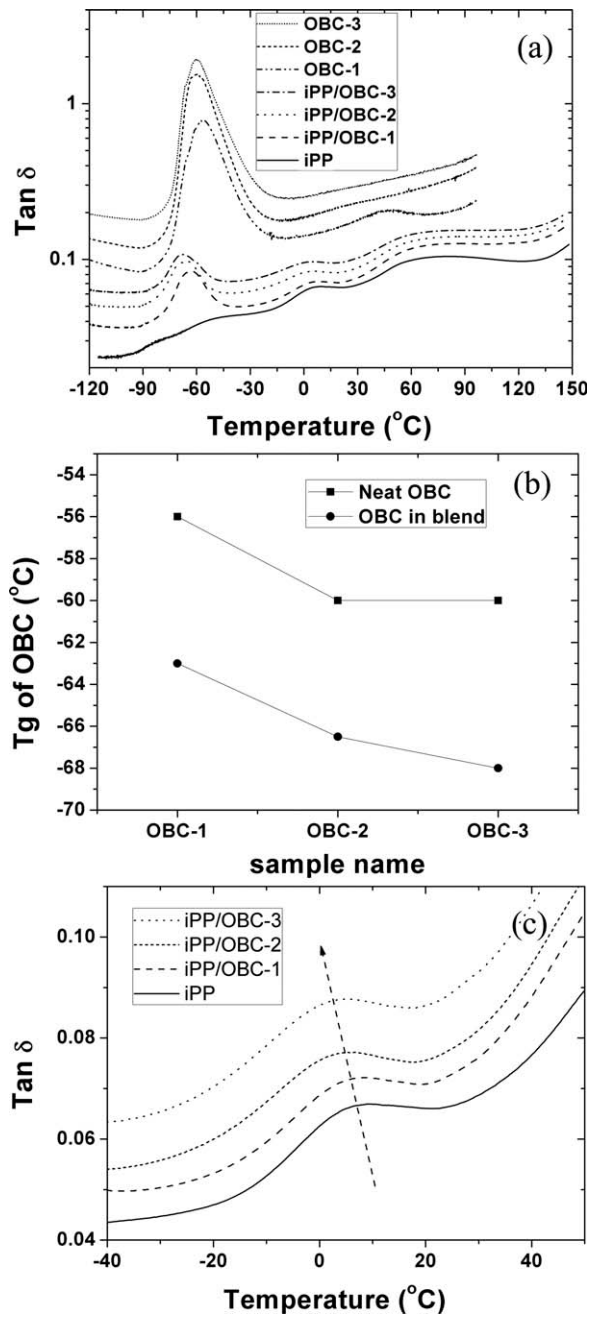

Figure 5 Dynamic mechanical behaviors of OBC and iPP/OBC blends: (a) Tan δ; (b) T_g of neat OBC and OBC in blend; (c) magnification of iPP glass transition zone. Curves in (a) and (c) are vertically shifted.

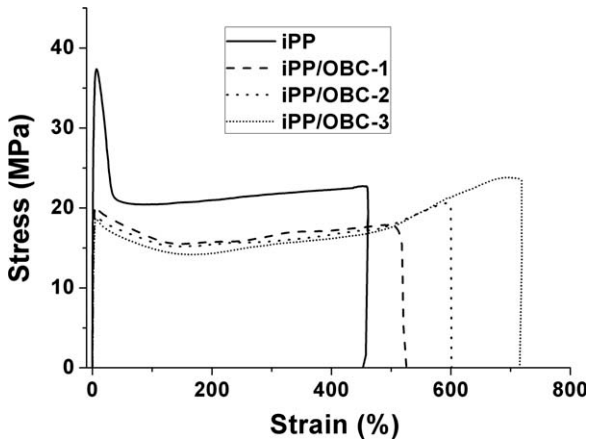

Figure 6 Engineering stress–strain curves of neat iPP and iPP/OBC blends.

iPP/EB, iPP/EH blends,[7] and iPP/EP blends.[8] However, it should be noted that the OBC in this study is a semicrystalline polymer. A recent study reported that OBC with 21 wt % hard segment showed strong scattering in SAXS.[31] Therefore, the data should be treated in a more precise manner by considering the contribution of the scattering of OBC.

The scattering curves of neat iPP and OBCs were superposed by considering the contribution of each component. As shown in Figure 4, the experimental curves of iPP/OBC blends were similar to the superposed curves of neat iPP and OBCs. Particularly, scattering curves of iPP/OBC-2 and iPP/OBC-3 were nearly the same as the superposed scattering curves. To quantitatively compare the experimental and superposed curves, the long spacing of the curves determined by the maxima in the Lorentz-corrected scattering curves were summarized in Table III. It was obvious that the superposed curves of iPP and OBC had the same line shape of iPP/OBC blends, indicating that the long spacing of iPP component in iPP/OBC was nearly the same as that of neat iPP. This result implies that iPP and OBCs seem to be immiscible.

Dynamic mechanical thermal analysis

DMTA is capable of determining the miscibility of two components in the amorphous region of polymer blends. A miscible binary blend will show one glass transition temperature (T_g) while an immiscible blend will show two separate T_gs located at the same positions as each component.[32,33] Partial miscibility is reflected by two T_gs in the blend, which are shifted toward each other, that is, the higher T_g is lowered and the lower T_g is increased simultaneously. The dynamic mechanical relaxation behaviors of iPP/OBC blends, neat OBC, and neat iPP are shown as Tan δ in Figure 5(a). A primary relaxation

TABLE IV
A Summary of the Relaxation Behavior of iPP and iPP/OBC Blends

	iPP	OBC-1	OBC-2	OBC-3	iPP/OBC-1	iPP/OBC-2	iPP/OBC-3
T_g of iPP (°C)	9.5 ± 0.1	–	–	–	8.2 ± 0.1	6.1 ± 0.1	5.4 ± 0.1
T_g of OBC (°C)	–	−56.5 ± 0.1	−60.3 ± 0.1	−60.3 ± 0.1	−63.3 ± 0.1	−66.6 ± 0.1	−68.2 ± 0.1

peak can be seen in neat OBC at about −60°C, which is conventionally identified as the β-relaxation in the amorphous phase. The β-relaxation is usually identified as the glass transition (T_g) of ethylene copolymers.[34,35] The crystalline α-relaxation at higher temperature was not observed due to the softening and flow of the material. Two primary relaxation peaks can be seen in neat iPP which are indentified as the crystalline α-relaxation and the β-relaxation of the amorphous phase.[35–37] Three primary relaxation peaks in iPP/OBC blends could be identified from high to low temperatures as crystalline α-relaxation of iPP, β-relaxation (T_g) of iPP, and β-relaxation (T_g) of OBC, respectively. The T_g of OBC in the blend is 7 ∼ 8°C lower than that of neat OBC [Fig. 5(b)]. T_g depression in a dispersed elastomer phase has been reported in iPP blending with elastomers such as random ethylene 1-butane copolymer (EB),[9] polystyrene-block-poly(ethene-*co*-1-butene)-block-polystyrene (SEBS), and random ethylene-octene copolymer (EO).[38] It has been proposed that the depression of T_g was attributed to the thermally induced internal stress resulting from differential volume contraction of the two phases during cooling from the melt.[38] The T_gs of the iPP component in blends were a little lower than that of neat iPP [Fig. 5(c)]. From iPP/OBC-1 to iPP/OBC-3, the T_gs of the iPP component decreased gradually, suggesting that the two components in iPP/OBC blends interacted and the interaction increased with the 1-octene content in the OBC soft segment.

It appears that the current iPP/OBC blends were partially miscible based on the shifted T_g of iPP component. However, the shift of T_g of the iPP component was small. Furthermore, the SAXS data showed that the iPP lamellae structure in the blends could be perfectly fitted by the combination of neat iPP and corresponding neat OBC scattering curves. To understand the somewhat confused experimental results, one should refer to the complex composition and unique chain structure of OBC. In addition to the molecular weight distribution, block length and the number of blocks distribution from multiblocks to diblocks, OBCs can contain hard segment rich and soft segment rich polymers.[39,40] In a recent study, it was suggested that the extraction of hard or soft segment rich polymers reduced the miscibility and broadened the partial miscible window of OBC/EO blends compared with the EO/EO blends.[17] Turning to this study, soft segment rich polymers could also play an important role in the miscibility of iPP/OBC blends. Because of the long ethylene segments in the hard OBC blocks, it is unlikely that multiblock component of OBC can be miscible with iPP. The soft segment rich polymers of the OBCs in this study, with high 1-octene content, could be partially miscible or miscible with iPP. According to the theoretical estimation of Lohse,[11] the miscibility window for iPP/EO at 167°C is about 55 to 70 wt % (∼ 23.4–36.8 mol %). Thus, the soft segment rich polymers in the tested OBCs could range from partially miscible to miscible with increasing the 1-octene content. Therefore, it is possible that these soft segment rich polymers could be incorporated into the iPP phase. This may explain the decreased T_g of iPP component in the blends. Noting that the fraction of soft segment rich polymers is about 8 ∼ 10 wt %,[17] the iPP T_g decrease is slight. Furthermore, one would expect that the small amount of extractable soft segments would have a trivial influence on the crystallization and melting behaviors of iPP. The net effect is that these iPP/OBC blends exhibit primarily the characteristic of immiscible blends. Assuming that the entire soft segment rich polymers could be incorporated in the amorphous of iPP, the long spacing of the iPP would only change about 5%, which is difficult to detect in quenched samples with a wide distribution of lamellar thicknesses.

TABLE V
Tensile and Flexural Properties of Neat iPP and iPP/OBC Blends

Sample name	Flexural modulus[a] (MPa)	Yield stress[b] (MPa)	Stress at break[b] (MPa)	Strain at break[b] (%)
iPP	1333 ± 4	35.4 ± 0.2	21.0 ± 2.	500 ± 120
iPP/OBC-1	759 ± 5	20.3 ± 0.2	18.3 ± 1.0	540 ± 50
iPP/OBC-2	710 ± 6	19.1 ± 0.2	20.0 ± 0.6	590 ± 40
iPP/OBC-3	625 ± 24	18.7 ± 0.1	23.1 ± 0.6	700 ± 50

[a] Determined from flexural tests.
[b] Determined from tensile tests.

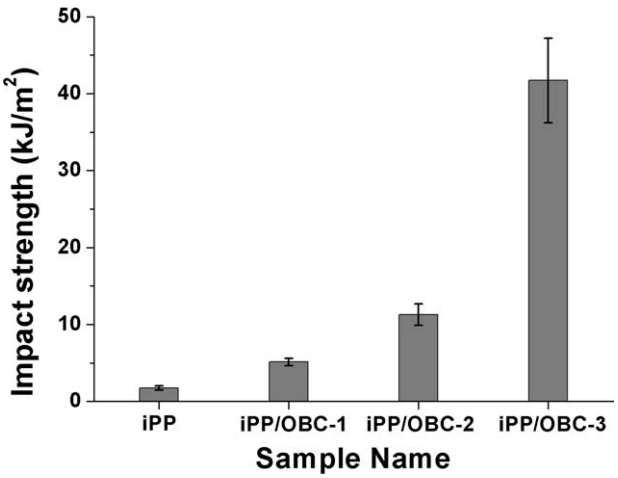

Figure 7 Room temperature Izod impact strength of iPP/OBC blends.

Mechanical properties

The engineering stress–strain curves obtained from tensile tests are plotted in Figure 6. As expected, the fracture strain increased and the yield stress deceased for the blends compared with neat iPP. Yielding became diffuse with the addition of elastomers. Furthermore, inclusion of elastomers promoted strain hardening phenomenon, and caused higher fracture strain, which agrees well with previous reports.[8,41,42] The effect of elastomer varied from OBC-1 to OBC-3, that is, the fracture stress and fracture strain increased from iPP/OBC-1 to iPP/OBC-3. Table IV summarizes the tensile and flexural experimental results. The modulus and yield strength of iPP/OBC blends were much lower than that of neat iPP and decreased from iPP/OBC-1 to iPP/OBC-3, which can be attributed to the different modulus of OBC component.

Notched Izod impact tests were performed at room temperature to evaluate the toughness of OBC with different soft segment 1-octene content (Fig. 7). Typically, neat iPP showed very poor impact toughness ($\sim$ 2 kJ/m^2). All the blends attained much higher impact strength than neat iPP, indicating that OBC can effectively enhance the toughness of iPP at room temperature. From iPP to iPP/OBC-2, the impact strength increased gradually. On the other hand, the room temperature impact strength for iPP/OBC-3 exhibited a sharply higher breaking energy compared with the other samples. In elastomer-toughened polymers, impact toughness was determined by elastomer particle size (interparticle distance) and interfacial adhesion.[1,43–45] It can be qualitatively observed from the SEM images that the elastomer phase size decreased in the blends from iPP/OBC-1 to iPP/OBC-3 (Fig. 1). It is likely that this decrease in average elastomer particle size enhanced the notched room temperature impact toughness of the blends.

To further understand the mechanism of different impact toughness of the iPP/OBC blends, SEM

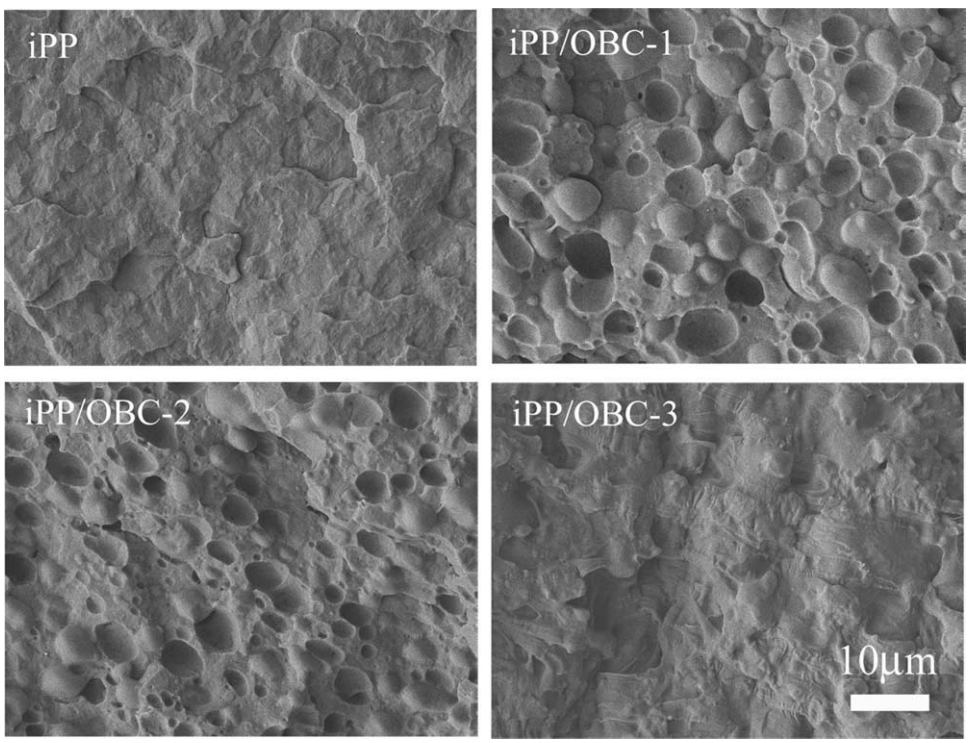

Figure 8 SEM images of fractured surface of iPP/OBC blends after Izod impact tests. The impact direction was from left to right.

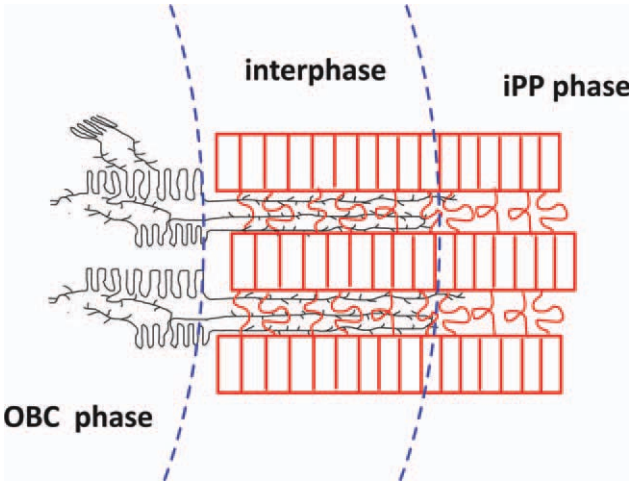

Figure 9 Schematic diagram of iPP/OBC interface structure. [Color figure can be viewed in the online issue, which is available at wileyonlinelibrary.com.]

observation of the fracture surface was performed (Fig. 8). For neat iPP, a sharp surface was observed which is in accordance with typical brittle fracture. Many holes and spheres in iPP/OBC-1 and iPP/OBC-2 fractured surface were shown, which is an indication of interfacial debonding. For iPP/OBC-3, distinct elongation deformation could be observed, and it is impossible to distinguish the matrix and dispersed elastomer, which is a typical characteristic of ductile fracture. The fracture morphology and impact strength data were well in accordance with each other.

Although it is likely that the miscibility of iPP/OBC blends was hindered by the crystallizable hard segments, the toughening effect varied significantly with increasing soft segment 1-octene content. This could be attributed to the higher compatibility arising from the higher interfacial adhesion between iPP/OBC and the resultant reduction in OBC particle size in the iPP matrix. Because of the increasing miscibility between iPP and soft segments from OBC-1 to 3, it is likely that they could more easily diffuse into the iPP phase during melt compounding, while the less compatible hard segments of OBC remained isolated in the OBC phase. A schematic diagram of the proposed iPP/OBC interaction is shown in Figure 9. The higher potential for soft segment diffusion for OBC with higher soft segment 1-octene content may have enhanced the interfacial adhesion between iPP and OBC. Thus, the sharp increase in the room temperature impact toughness of iPP/OBC-3 could be attributed to both the small elastomer particle size and strong interfacial adhesion.

CONCLUSIONS

The development and commercialization of OBCs offer new opportunities for polyolefin blends and create a need for understanding their effectiveness on polymer toughening. In the present study, we systematically investigated the miscibility of iPP/OBC blends with varied 1-octene contents in the soft segment of OBC and their corresponding mechanical properties. It is evident that the investigated OBCs were immiscible with iPP at all 1-octene levels in the soft segment. However, due to the existence of soft segment rich polymers in the OBCs, this portion of the OBCs composition may exhibit partial miscibility with iPP, leading to slight iPP T_g depression. The mechanical properties especially the room temperature impact toughness were greatly increased as the OBC soft segment 1-octene increased. It is believed that the enhanced mechanical properties were due to the increase in iPP/OBC interfacial bonding as the OBC soft segments 1-octene content increased, resulting in substantially higher iPP/OBC adhesion and smaller particle size in the iPP matrix.

References

1. Jang, B. Z.; Uhlmann, D. R.; Vandersande, J. B. Polym Eng Sci 25, 643, 1985.
2. Yokoyama, Y.; Ricco, T. Polymer 39, 3675, 1998.
3. Jang, B. Z. J Appl Polym Sci 30, 2485, 1985.
4. Liang, J. Z.; Li, R. K. Y. J Appl Polym Sci 77, 409, 2000.
5. Bensason, S.; Minick, J.; Moet, A.; Chum, S.; Hiltner, A.; Baer, E. J Polym Sci Part B: Polym Phys 34, 1301, 1996.
6. Bensason, S.; Nazarenko, S.; Chum, S.; Hiltner, A.; Baer, E. Polymer 38, 3913, 1997.
7. Yamaguchi, M.; Miyata, H.; Nitta, K. H. J Appl Polym Sci 62, 87, 1996.
8. Nitta, K. H.; Shin, Y. W.; Hashiguchi, H.; Tanimoto, S.; Terano, M. Polymer 46, 965, 2005.
9. Maeder, D.; Thomann, Y.; Suhm, J.; Mulhaupt, R. J Appl Polym Sci 74, 838, 1999.
10. Schweizer, K. S.; Singh, C. Macromolecules 28, 2063, 1995.
11. Lohse, D. J. J Macromol Sci: Polym Rev 45, 289, 2005.
12. Arriola, D. J.; Carnahan, E. M.; Hustad, P. D.; Kuhlman, R. L.; Wenzel, T. T. Science 312, 714, 2006.
13. Lejiv, M.; Maurer, F. H. J. Polym Eng Sci 28, 670, 1988.
14. Zhou, X. Q.; Hay, J. N. Polymer 34, 4710, 1993.
15. Bains, M.; Balke, S. T.; Reck, D.; Horn, J. Polym Eng Sci 34, 1260, 1994.
16. Flaris, V.; Zipper, M. D.; Simon, G. P.; Hill, A. J. Polym Eng Sci 35, 28, 1995.
17. Kamdar, A. R.; Wang, H. P.; Khariwala, D. U.; Taha, A.; Hiltner, A.; Baer, E. J Polym Sci Part B: Polym Phys 47, 1554, 2009.
18. Liu, G. M.; Zhang, X. Q.; Liu, C. Y.; Chen, H. Y.; Walton, K.; Wang, D. J. J Appl Polym Sci 119, 3591, 2011.
19. Wu, S. H. Polym Eng Sci 27, 335, 1987.
20. Favis, B. D.; Willis, J. M. J Polym Sci Part B: Polym Phys 28, 2259, 1990.
21. Lepers, J. C.; Favis, B. D.; Tabar, R. J. J Polym Sci Part B: Polym Phys 35, 2271, 1997.
22. Clark, E. J.; Hoffman, J. D. Macromolecules 17, 878, 1984.
23. Li, L. B.; Zhang, L. J Polym Sci Part B: Polym Phys 44, 1188, 2006.
24. McNally, T.; McShane, P.; Nally, G. M.; Murphy, W. R.; Cook, M.; Miller, A. Polymer 43, 3785, 2002.
25. Dong, L.; Olley, R.; Bassett, D. J Mater Sci 33, 4043, 1998.

26. Manaure, A. C.; Muller, A. J. Macromol Chem Phys 201, 958, 2000.
27. Prieto, O.; Perena, J. M.; Benavente, R.; Cerrada, M. L.; Perez, E.; Macromol Chem Phys 203, 1844, 2002.
28. Hu, S. R.; Kyu, T.; Stein, R. S. J Polym Sci Part B: Polym Phys 25, 71, 1987.
29. Ree, M.; Kyu, T.; Stein, R. S. J Polym Sci Part B: Polym Phys 25, 105, 1987.
30. Bedia, E. L.; Murakami, S.; Senoo, K.; Kohjiya, S. Polymer 43, 749, 2002.
31. Zuo, F.; Burger, C.; Chen, X.; Mao, Y.; Hsiao, B. S.; Chen, H. Y.; Marchand, G. R.; Lai, S. Y.; Chiu, D. Macromolecules 43, 1922, 2010.
32. Schneider, H. A. In Polymeric Materials Enyclopedia; Salomone, J. C., Ed.; CRC Press: Boca Raton, FL, 1996; p 2777.
33. Schneider, H. A. J Res Natl Inst Stand Technol 102, 229, 1997.
34. Popli, R.; Glotin, M.; Mandelkern, L.; Benson, R. S. J Polym Sci Part B: Polym Phys 22, 407, 1984.
35. Boyd, R. H. Polymer 26, 1123, 1985.
36. Boyd, R. H. Polymer 26, 323, 1985.
37. Jourdan, C.; Cavaille, J. Y.; Perez, J. J Polym Sci Part B: Polym Phys 27, 2361, 1989.
38. Maeder, D.; Bruch, M.; Maier, R. D.; Stricker, F.; Mulhaupt, R. Macromolecules 32, 1252, 1999.
39. Shan, C. L. P.; Hazlitt, L. G. Macromol Symp 257, 80, 2007.
40. Anantawaraskul, S.; Somnukguande, P.; Soares, J. B. P. Macromol Symp 282, 205, 2009.
41. Yang, J. H.; Zhang, Y.; Zhang, Y. X. Polymer 44, 5047, 2003.
42. Pang, Y. Y.; Dong, X.; Zhang, X. Q.; Liu, K. P.; Chen, E. Q.; Han, C. C.; Wang, D. J. Polymer 49, 2568, 2008.
43. Wu, S. H. Polymer 26, 1855, 1985.
44. Wu, S. H. J Appl Polym Sci 35, 549, 1988.
45. Corte, L.; Leibler, L. Macromolecules 40, 5606, 2007.